Journal of Sciences, Islamic Republic of Iran 29(2): 129 - 142 (2018) http://jsciences.ut.ac.ir
University of Tehran, ISSN 1016-1104

Petrography, Major and Trace Elemental Geochemistry of the Ordovician-Silurian Siliciclastics in North of Tabas Block, Central Iran: Implications for Provenance and Paleogeography

E. Khazaei[1], M.H. Mahmoudy-Gharaie[1], A. Mahboubi[1*]
R. Moussavi-Harami[1], J. Taheri[2]

[1] *Department of geology, Faculty of Sciences, Ferdowsi University of Mashhad, Mashhad, Islamic Republic of Iran*
[2] *Geological Survey of Iran, Mashhad Branch, Mashhad, Islamic Republic of Iran*

Received: 20 February 2017 / Revised: 7 May 2017 / Accepted: 14 June 2017

Abstract

The upper part of Shirgesht (UPS) and lower part of Niur (LPN) formations (Ordovician-Silurian) consist of sandstone, shale and limestone, respectively. The petrography and geochemical analysis conducted to evaluate provenance of siliciclastic deposits in order to understand the paleogeography of Central Iran during the Early Paleozoic time. This study shows that quartz and K-feldspar are the most abundant minerals in these siliciclastic rocks and the felsic igneous rock, probably granite, is the possible source rock. The average CIA (71) value and rare earth elements diagram, such as Th/U ratio versus Th, reveal a high degree of paleo-weathering in the source area. The craton interior and transitional continent were interpreted as a tectonic setting for UPS and LPN formations, respectively. Furthermore, the geochemical analysis revealed active continental margin and mostly passive margin during deposition of these two formations, respectively. Rifting in Central Iran during Ordovician-Silurian time generated normal faults at the edge of platform which had a major role in production of siliciclastic deposits.

Keywords: Shirgesht and Niur formations; Provenance; Petrography; Geochemistry; Tectonic setting.

Introduction

Mineralogical and geochemical properties of siliciclastic rocks are depending upon some factors such as tectonic setting, source rock, weathering intensity, transport, depositional processes and diagenesis. The first and second one has known as two major controlling factors during generation of siliciclastic sediments [1]. Based on petrographical analysis, several models have been used for interpretation of provenance parameters (e.g. lithology of source area, climate, weathering and tectonic setting) [2-6]. In recent years, geochemical data were significantly used as a tool for interpretation of provenance [7-14]. The provenance of siliciclastic rocks

* Corresponding author: Tel: +989155128018; +985138805484; Fax: +985138796416; Email: mahboubi@um.ac.ir

included all of efficient factors that have important role in sediments supply together with physiography and climatic conditions at the source area. Trace elements (e.g. Nb, Ni, V, Co, Y, La, Th, Zr) in sediments are stable versus weathering, diagenesis and moderate stage of metamorphism [15]. Therefore, these elements can also be used to interpret provenance properties and tectonic setting [15-21]. The Silurian Shirgesht Formation has been studied by various researchers in Central Iran [22, 23]. Bayetgol [24] studied depositional environment and diagenesis of Shirgesht Formation in Asheghan and Kuh-e-Radar in Central Iran. Nowrouzi et al. [25] interpreted sedimentary environment of Niur Formation in Central Iran. Saheb Jamei [26] studied Shirgest and Nur Formations at studied locality to determine the age of these strata based on palynology and palynostratigraphy. However, they did not consider sedimentological aspects of the Ordovician-Silurian deposits at the studied area. Therefore, the main purpose of this research is to interpret provenance, tectonic setting of the Upper Ordovician-Lower Silurian deposits (upper part of Shirgesht- lower part of Niur formations) (UPS-LPN) in Central Iran tectono-sedimentary zone. We believe these data can lead to a better understanding of the Early Paleozoic paleogeography of the region.

Geological setting

Microplate of Central Iran is a structural unit with north-south trend and consists of three blocks including Loot, Tabas and Yazd (Fig. 1). For the first-time, Rutner et al [27] studied the Ordovician rocks in the Shirgesht area and named the Shirgesht Formation for Ordovician and Niur Formation for Silurian rocks in SE Ozbak Kuh. The Shirgesht Formation with 1236 m thickness is the thickest Ordovician successions in Iran. This Formation consists mainly of sandstone and shale with limestone interbeds at the type section. The Niur Formation at the type locality is composed of brown limestone with shale and dolostone interbeds in lower part.

The Silurian succession in Central Iran, particularly in Jam, Taroud, north of Bafgh, Anarak and Kashan, has recorded evidence of Caledonian orogeny. The study area is called Kuh-e-Boghou and is located in north of Tabas Block (Fig. 1). This section is composed of sandstone and shale of the upper part of Shirgesht Formation with 135m thickness and shale with

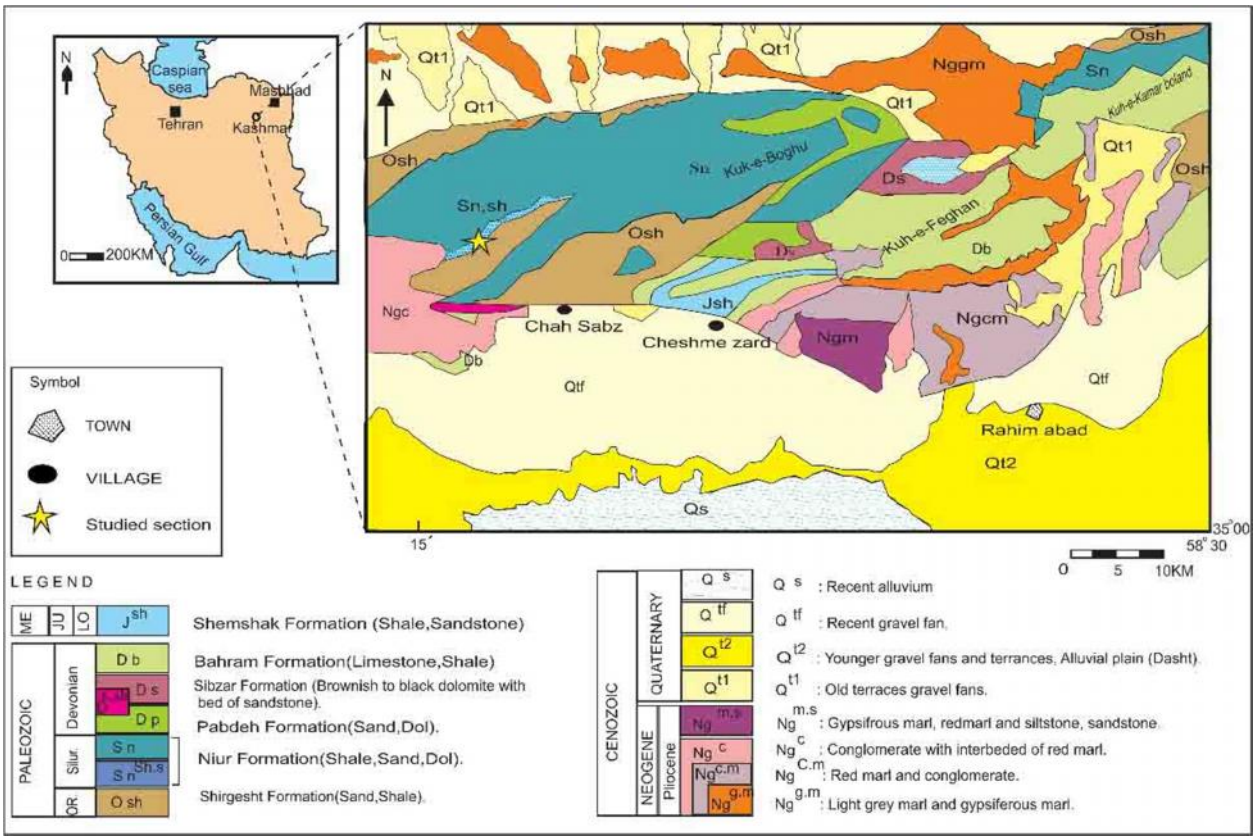

Figure 1. Location of measured section is shown by star in Tabas Block (modified from Taheri [29]).

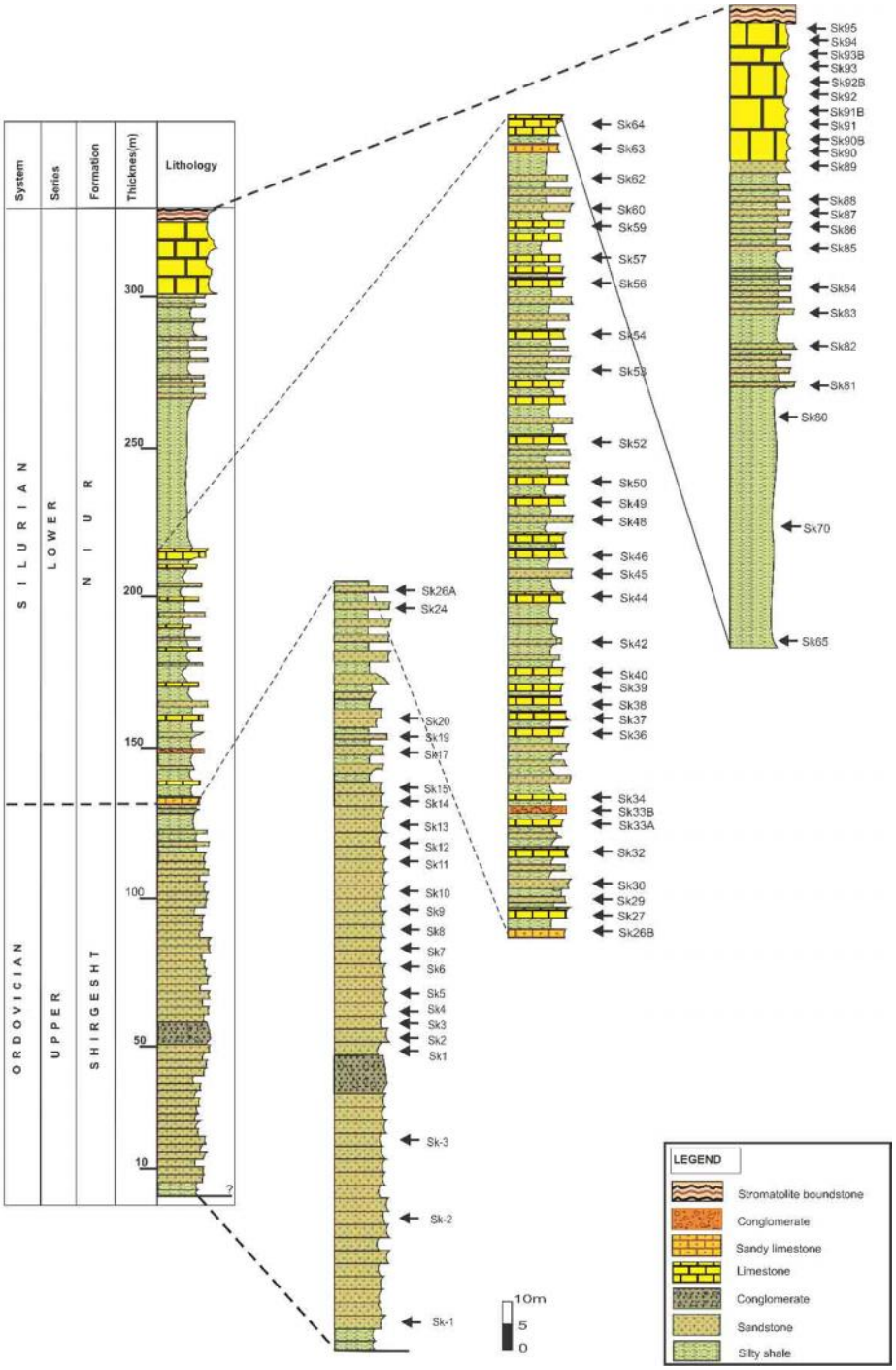

Figure 2. Lithostratigraphy column of the UPS and LPN formations in Kuhe-Boghu north of Tabas block. The location of samples are shown in the column.

sandstone and limestone interbeds of Niur Formation with 200m thickness that are Upper Ordovician and Lower Silurian in age respectively [28]. The lower boundary of Shirgesht Formation is faulted, while contact between Shirgesht and Niur formations is gradational (Fig. 2).

Materials and Methods

This study was done based on one measured stratigraphic section. 26 samples from the UPS and 20 samples from the LPN formations were collected. In each sandstone thin section, 300 to 400 grains were counted for modal analysis and classified based on

Pettijohn et al [classification scheme [30]. Geochemical analysis carried out on eight sandstone and 11 shale samples for determination of major, trace and rare earth elements (REE) based on analysis by ICP-AES in the laboratory of the Geological Survey of Iran.

Results

Petrography and Modal analysis

The sandstones of UPS Formation are fine grain, angular to subrounded, moderately sorted and contain more than 15% matrix. The sandstones of LPN Formation are fine-grained, subrounded and poorly sorted. Quartz (75 to 85%) and feldspar (15 to 20%) are the major grains types in these sandstones (Table 1). Both monocrystalline (Qm) and polycrystalline quartz (Qp) present in studied samples; however, monocrystaline quartz with undulose extinction is the most abundant grain (Fig. 3). Feldspar grains include alkali and plagioclase, but muscovite and zircon grains are present too (Fig. 3) (Table 1). Based on Pettijohn et al [30] classification scheme, these sandstones are arkosic wacke and subarkose for UPS and LPN formations, respectively (Fig. 4).

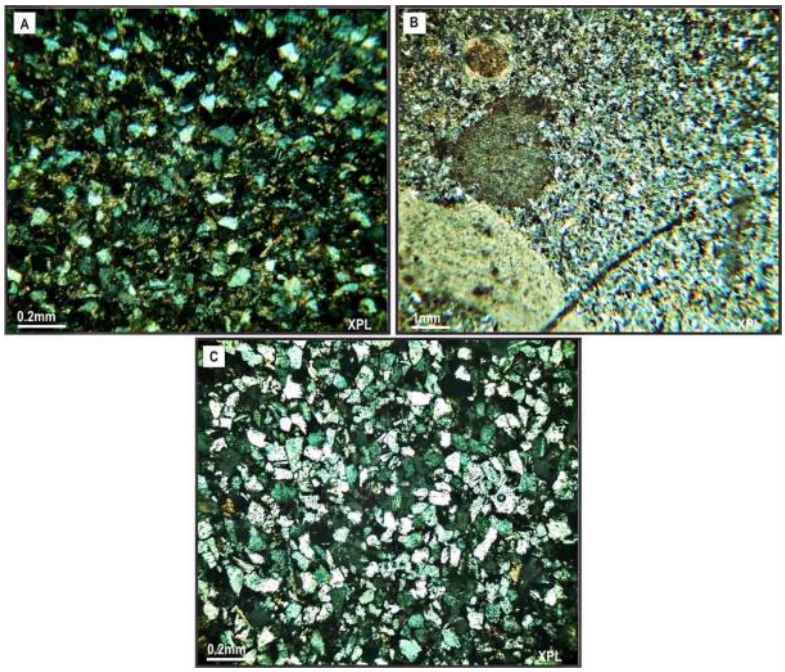

Figure 3. Sandstones petrofacies: A) Arkosic wacke, B) Arkosic wacke with fossil fragments, C) Subarkose.

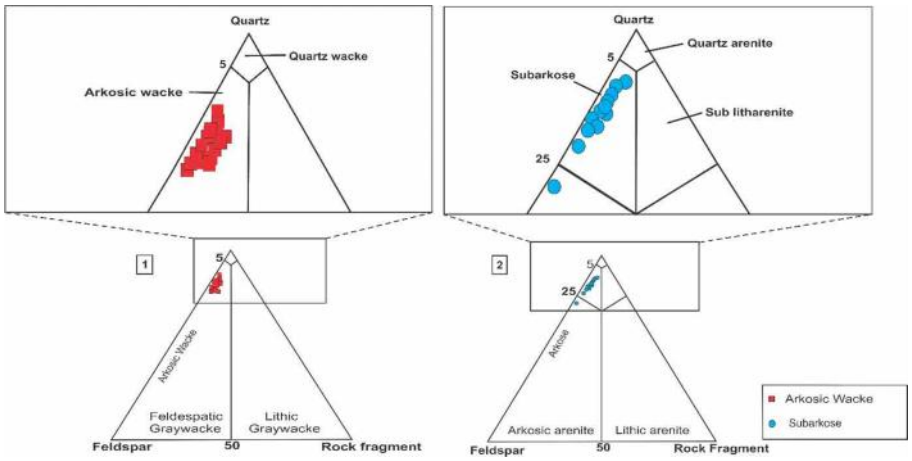

Figure 4. Sandstone modal data on the triangle of Pettijohn et al [30]. 1: Shirgesht Fm, 2: Niur Fm.

Table 1. Modal analysis data of the studied sandstones.

Formation	Petrofacies	Sample.No	Q_{pq}	$Q_{pq>3}$	Q_m	$Q_{m\ un}$	$Q_{m\ non}$	Q_t	K	P	L_s	Cht	L_t
Shirgesht	Arkosic wacke	SK-1	22.5	22.3	41.6	11.1	30.4	86	10.2	3	0	0.5	0.5
		SK-2	24.7	21.2	34.5	7.9	26.5	80.5	13.2	6.1	0	0	0
		SK-3	23.4	22.2	39.5	6.2	33.3	85.1	14.8	6.1	0	0	0
		SK1	20	18	42	12	30	80	13	4	0	0.5	0.5
		SK2	21	20	43	15	28	84	11	5	0	0	0
		SK3	20.5	16.5	43	13	30	80	18	2	1	1	2
		SK4	17	15	46	6	40	78	18	4	0	0	0
		SK5	20.3	19.2	41.5	10	31.5	81	15	3	0	1	1
		SK6	5.2	1.5	78	18.5	59.5	84	12.1	2.9	0.5	0.5	1
		SK7	15	10	40	10	30	75	19	4	0	2	2
		SK8	10	7	68	22.9	45.8	85.9	10.3	3.6	0	0	0
		SK9	7.9	6	73	12.7	60.7	87.5	10.9	1.5	0	0	0
		SK10	12.9	8.1	62.1	18.9	43.2	83.2	13.5	3.2	0	0	0
		SK11	15.3	9.2	56.5	10.4	46.1	81	14	5	0	1	1
		SK12	17.5	6.7	53.2	9.8	43.4	77.4	18.2	4.2	0	0	0
		SK13	13.3	8.7	63	9.9	53	83	14.5	2.1	0	0	0
		SK14	9.3	12.2	55.1	11.9	43.1	76.6	16.9	6.3	0	0	0
		SK15	16.7	8.9	49	10.1	38.9	74.7	23.7	1.5	0	0	0
		SK119	18	12	50	15	35	80	15	3	0.5	1	2
		SK20	20.7	4.9	57.6	16.1	41.4	83.4	14.5	2	0	0	0
Niur	Subarkose	SK24	14	10	54	19	35	78	18	4	0	0	0
		SK26	16	11.5	53.5	14	39.5	81	15	3	1	0	1
		SK29	25	6	49	9	40	80	17	3	0	0	0
		SK30	9.3	19	49.7	9.3	40.4	78.1	18.6	2.7	0	0.5	0.5
		SK38	16.2	8.1	65.1	28.1	37	89.6	7.4	2.9	0	0	0
		SK42	15	11	55	19	36	81	16	3	0	0	0
		SK53	19.8	9.9	57.6	12.6	45	87.3	9	3.6	0	0	0
		SK60	26.3	20.8	40.2	13.8	26.3	87.5	9.7	2.7	0	0	0
		SK63	23.8	15.4	51.1	13	38	90.4	7.1	2.3	0	0	0
		SK83	22	16	53	7.5	45.5	92.4	4.5	2.5	0	0.5	0.5
		SK84	10	4.2	72.8	21.4	51.4	88.5	7.8	3.5	0	0	0
		SK85	25	10	53	18	35	88	8	4	0	0	0
		SK86	26	18	41.4	9.5	9.5	86.1	10.6	3.6	0	0	0
		SK87	27.7	14.5	31.2	6.9	24.3	73.6	20.8	5.5	0	0	0
		SK88	26.6	14.2	40.9	7.6	33.3	81.9	14.2	3.8	0	0	0
		SK89	16	9.9	61.1	20	41.1	79	17	4	0	0	0

Geochemistry

Major elements

The major elements values are provided in Table 2. SiO_2 has the highest value with 60 to 72 (Wt.%). Al_2O_3 is the second element ranging from 12.7 to 22.9 %. The logarithmic relationship of K_2O/Na_2O versus SiO_2/Al_2O_3 shows that sandstones of UPS and LPN formations are arkosic wacke and subarkose, respectively (Fig. 5) as shown by petrography studies too.

The trace elements concentrations of the studied samples are presented in Table 3. In general, the frequency of specific major and trace elements can indicate the dominant mineralogy of components in sandstones. The mean values of LILE (large-ion lithophile elements), including Rb, Th, U, Sr and Ba are 120.4, 36.7, 6.3, 110.8 and 325 ppm respectively. The trace elements of the chondrite normalized curves (Fig. 6) show that Rb, Sr and Ba are enriched relative to Upper Continental Crust (UCC) [31, 32], while, U depleted. The mean values of HFSE **(**High Field Strength Elements**),** including Zr, Nb and Hf are 341, 37 and 4.9 ppm, respectively. So, the studied samples enriched in Zr and depleted in Hf elements (Fig. 6). The

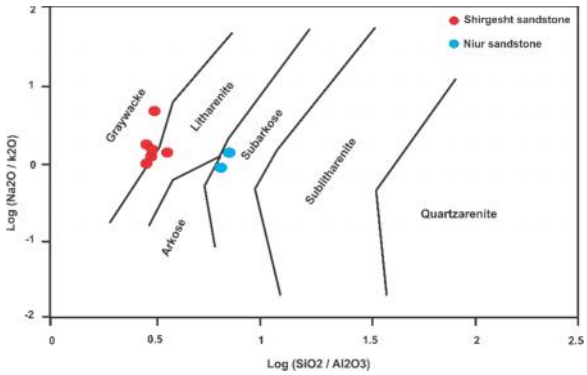

Figure 5. Geochemical classification diagram of sandstones based on log (SiO_2/Al_2O_3) versus log (Na_2O/K_2O) (After Pettijohn et al [30]). The studied samples are plotted on subarkose and greywacke fields.

Table 2. Major element oxides values (%) for UPS and LPN formations.

Formation	Sample NO.	SiO_2	Al_2O_3	Fe_2O_3	MgO	CaO	Na_2O	K_2O	TiO_2	P_2O_5	MnO	Cr_2O_3
Shirgesht	Sk-1	70.1	13.5	6.8	1.3	0.2	2	5.1	1.4	0.01	0.01	0.03
	Sk-2	71.1	14	5.1	1.3	0.6	2.5	4.7	0.9	0.02	0.01	0.01
	Sk-3	73.4	13.7	3.4	1.3	0.5	2.6	4.4	1.01	0.02	0.01	0.01
	Sk8	67.7	15.9	6.6	1.3	0.3	4.4	2.9	1.1	0.02	0.01	0.02
	Sk13	69	14.5	7.1	1.1	0.3	2.4	4.5	1.2	0.01	0.01	0.01
	Sk17	72	14.9	2.9	0.3	0.3	1.2	7.2	1.6	0.09	0.008	0.02
Niur	Sk21	63.4	19.3	7.6	1.8	0.1	1.6	5	1.4	0.05	0.02	0.01
	Sk23	62.4	17.3	11.4	1.6	0.2	2.8	3.1	1.6	0.07	0.02	0.02
	Sk30	66.6	15.4	9.3	1.5	0.3	1.2	4.5	1.6	0.02	0.02	0.01
	Sk35	62.8	19.3	8	1.9	0.3	2.6	3.9	1.6	0.03	0.02	0.02
	Sk41	61.5	20.5	8	2.1	0.1	1.8	4.7	1.5	0.03	0.02	0.02
	Sk47	60.8	21.5	7.4	2.1	0.1	1.6	5.2	1.6	0.03	0.02	0.02
	Sk51	60.6	21.1	8.1	2.3	0.2	2.1	4.5	1.4	0.04	0.02	0.02
	Sk61	63	19.8	7.7	1.8	0.3	3	3.4	1.2	0.03	0.02	0.02
	Sk66	60.4	22.9	6.6	2.1	0.1	1.9	5	1.3	0.02	0.02	0.01
	Sk69	60.5	22.1	7.8	2.2	0.1	1.7	4.6	1.3	0.01	0.02	0.03
	Sk75	61.9	20.7	7.9	2.2	0.2	2.2	3.9	1.3	0.05	0.03	0.02
	Sk80	66.3	18.1	6.6	1.4	0.3	3	3.4	1.1	0.03	0.02	0.01
	Sk83	72.8	12.7	7.5	0.8	0.2	1.8	3.7	1.05	0.01	0.02	0.02

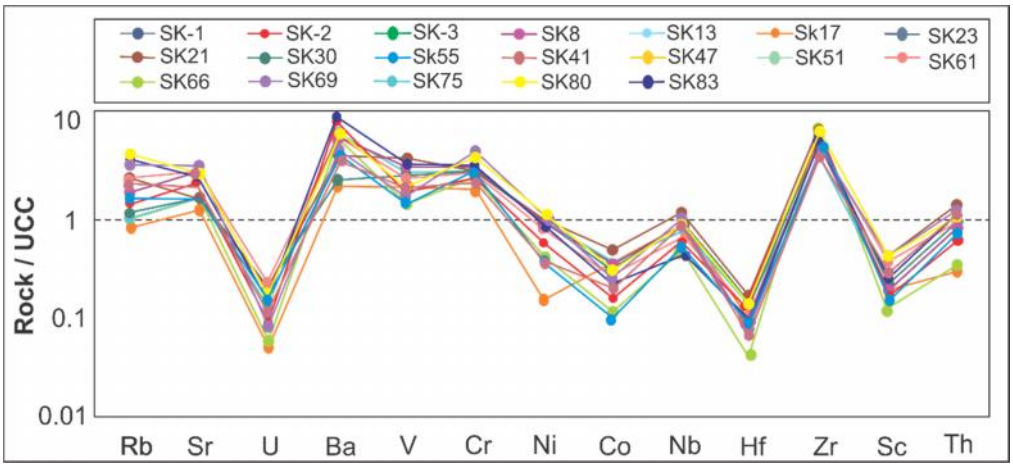

Figure 6. Spider diagram of Chondrite-normalized trace elements of the studied samples from UPS and LPN formations.

mean values of FTE (ferromagnesian trace elements), including Co, Cr, Ni, Sc and V are 13.4, 147, 36, 13.7 and 130.1 ppm, respectively. The Cr and Co enriched relative to UCC and Ni has almost similar value to UCC (Fig. 6). Enrichment of Cr can be related to mafic or ultramafic materials and maybe related to Eh conditions; therefore cannot be used for provenance interpretation.

Discussion

Source area paleo-weathering

The chemical index of alteration (CIA) is an efficient method for assessment of weathering intensity in source area [33]. The CIA is expressed as CIA= [Al_2O_3/ (Al_2O_3+CaO+Na_2O+K_2O)] ×100, where Al_2O_3, CaO, Na_2O, and K_2O are in molar proportion, and CaO is restricted to the calcium derived from silicate minerals [33]. The CIA index values can be varied based on alteration intensity of feldspars. The CIA values between 50 and 60 indicative of a low degree, while the values between 60 and 80 show moderate and values more than 80 represent high intensity weathering in the source area.

The calculated CIA values show variations from 63.12 to 67.5 for UPS (with average of 65) and from 69.5 to 77 (with average of 74) for LPN deposits. Therefore, the average CIA suggests that the source rocks suffered moderate weathering [33] (Fig. 7). In addition, the ratios of some rare earth elements, such as

Table 3. Trace element values (ppm) for UPS and LPN formations.

Fm	Sample no.	Rb	Sr	Ba	Pb	Th	U	Hf	Zr	Nb	Sc	V	Cr	Co	Ni	Zn
Shirgesht	Sk-1	49.4	74.0	294	3.6	33.9	6.8	5.1	264	26.3	6.0	96.6	223	8.3	17.8	48.1
	Sk-2	66.9	105	376	4.3	26.6	4.9	3.7	385	30.9	6.9	82.5	121	7.4	27.6	50.2
	Sk-3	72.3	107	393	3.0	17.0	2.9	5.3	234	20.2	5.8	64.5	118	5.8	18.9	43.6
	Sk8	87.5	136	478	8.2	32.2	5.9	<2	242	27.8	9.1	122	119	12.4	35.5	88.1
	Sk13	70.1	114	365	7.2	36.7	7.2	5.3	240	26.4	8.8	122	157	13.4	42.4	65.6
	Sk17	37.9	56.8	100	10.0	14.3	2.3	<2	443	38.0	9.0	101	93.1	16.5	7.2	19.3
	Sk21	189	113	467	5.4	39.7	6.0	5.3	333	42.5	19.1	154	146	9.7	35.4	76.2
	Sk23	121	68.6	192	13.8	63.4	10.8	8.5	462	54.8	15.6	188	135	22.3	44.9	83.2
	Sk30	52.8	73.2	118	12.2	48.1	10.0	4.3	533	53.9	10.8	146	148	17.1	47.9	76.9
	Sk35	148	125	352	77.8	41.3	7.2	4.0	376	38.7	17.4	144	157	13.3	46.4	73.3
	Sk41	181	115	385	3.6	40.5	6.7	6.0	329	44.8	20.0	152	141	13.8	42.1	77.9
Niur	Sk47	201	128	411	3.9	38.3	5.4	5.8	382	45.4	20.7	182	162	12.7	39.4	77.0
	Sk51	178	133	362	4.4	42.4	6.9	6.6	414	43.2	19.2	152	140	17.1	43.2	90.2
	Sk61	125	144	320	3.1	38.9	6.9	5.3	275	34.1	16.9	122	128	15.6	37.7	79.7
	Sk66	188	141	363	5.8	31.9	5.3	2.1	472	55.3	15.4	161	216	12.2	63.7	79.4
	Sk69	176	132	359	8.3	39.4	6.2	4.9	320	40.5	19.7	161	165	15.0	41.9	88.4
	Sk75	152	127	329	7.2	42.2	6.7	2.1	217	32.3	17.9	139	142	19.8	46.5	94.2
	Sk80	120	137	287	5.1	33.2	5.3	5.2	261	27.8	15.3	120	128	10.3	28.9	60.4
	Sk83	70.8	76.6	214	8.5	37.6	6.7	4.3	288	19.4	7.0	62.8	145	11.2	17.4	49.2

Th/U, can be used for identification of intensity of chemical weathering in source rocks. The mean ratio of Th/U in studied samples is 5.95. Plotting data on McLennan [34] diagram show that the weathering increased at the source area (Fig. 8). This indicates that sediments derived from a source area with moderate degree of weathering.

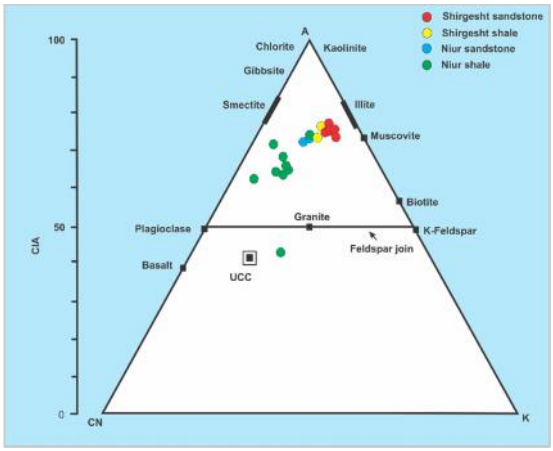

Figure 7. Plot of major oxide in A-CN-K diagram [33]. The studied samples show a trend from plagioclase to intense weathering in illite area.

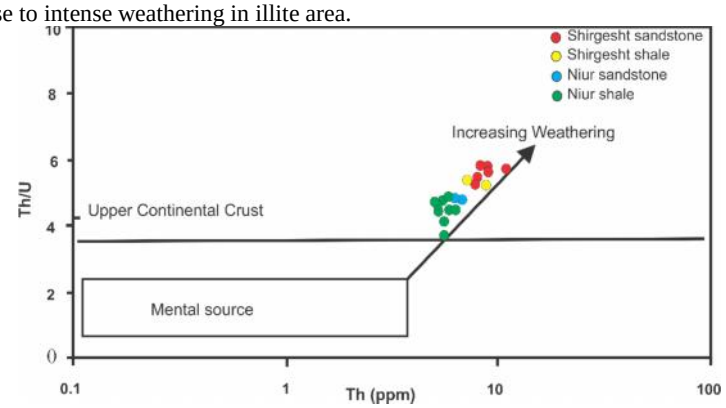

Figure 8. Th/U versus Th diagram that illustrating weathering trend (after McLennan [34]).

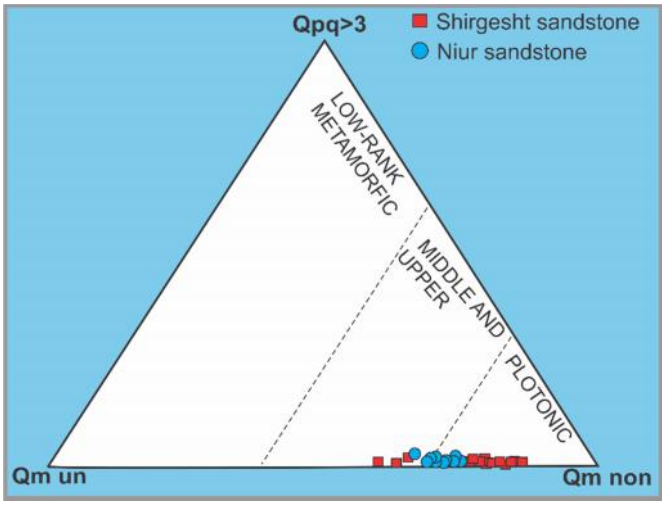

Figure 9. Possible source rock for studied area based on quartz characteristics (after Basu et al [36]).

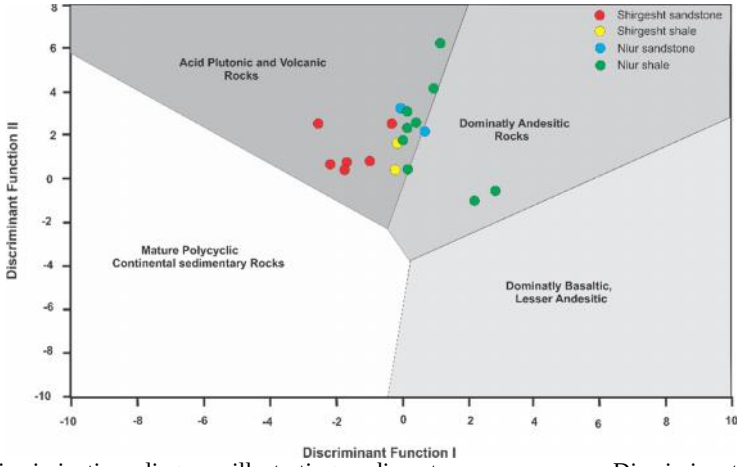

Figure 10. Discrimination diagram illustrating sedimentary provenance. Discriminant function (DF) analysis using major elements (after Roser & Korsch [37]).

Source rock

Present of monocrystalline undulose quartz with zircon and muscovite suggest a plutonic igneous source rock [32, 35]. Based on optical characteristics of monocrystalline and some polycrystalline quartz [36], they may have derived mainly from plutonic igneous rocks (Fig. 9).

In the other hand, using the functional diagram based on major oxides [37] (Fig. 10) showed acidic plutonic rock. The La/Co، Th/Sc، La/Sc and Th/Co ratios (Table 4), as well as logarithmic relationship of Th/Sc versus Zr/Sc, La/Sc versus Th/Co [38] (Fig. 12), and Ni-V-Th×10 diagram [39] (Fig. 13) show that a possible felsic rock (such as granite) can be a source for the components of UPS and LPN siliciclastic deposits.

Tectonic setting

The various tectonic settings contain different sedimentary rocks; therefore they produce distinctive sandstones with exceptional components when they

Table 4. Elemental ratios, compared to UCC

Elemental Ratio	UCC**	Range Of Sediment From Mafic Rocks**	Range of Sediment From Felsic Rocks**	Studied Samples
La/Sc	2.21	0.43-0.86	2.5-16.3	1.08-6.98
Th/Sc	0.79	0.05-0.22	0.84-20.5	1.58-5.65
La/Co	1.76	0.14-0.38	1.80-13.8	0.65-6.98
Th/Co	0.63	0.04-1.40	0.65-19.4	0.85-4.09

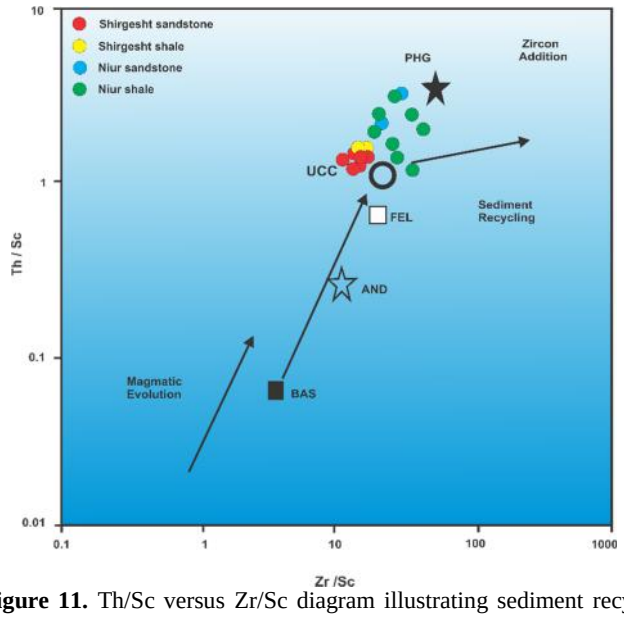

Figure 11. Th/Sc versus Zr/Sc diagram illustrating sediment recycling (after McLennan [34]). Samples are mostly located close to UCC area.

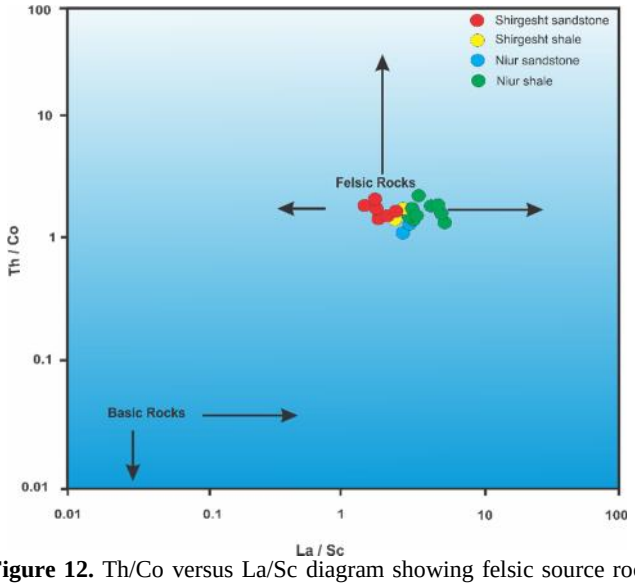

Figure 12. Th/Co versus La/Sc diagram showing felsic source rock for studied siliciclastic sediments (after Cullers [38]).

undergo weathering conditions. Plotting of modal analysis data on the Qm-F-L ternary diagram [40] indicates the cratonic interior and transitional continental tectonic settings for UPS and LPN, respectively (Fig. 14). Based on Dickinson et al. [40], our samples are plotted in the range of craton interior and can be derived from granitic or older quartzose sedimentary source rock. These possible source rocks were exposed in the craton interior. It should keep in mind that diagenesis can change the composition of rocks, therefore this can change the location of plotted data on the Q-F-L. Nevertheless, the comprehensive evaluation in relative to all of factors is necessary for provenance studies. Also, various researchers used geochemical data to support the petrography in order to interpret provenance of sandstones [15, 37,41].

In our study, two methods were used as geochemical approaches for interpretation of tectonic setting. In the plots of K_2O/ Na_2O versus Si_2O, based on major oxides, most samples are plotted on active continental margin area (Fig. 15). Using the ternary diagrams of Th–Co–Zr/10 and Th–Sc–Zr/10 [15] also show that the UPS Formation samples located in the active continental margin area, while LPN Formation samples indicating

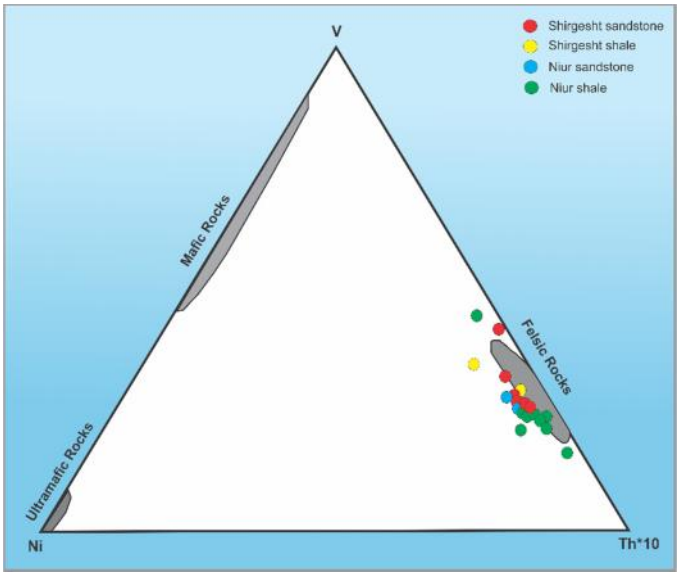

Figure 13. Ternary diagram of V-Ni-Th*10 showing felsic source rock for studied siliciclastic sediments (after Braccialli et al [39]).

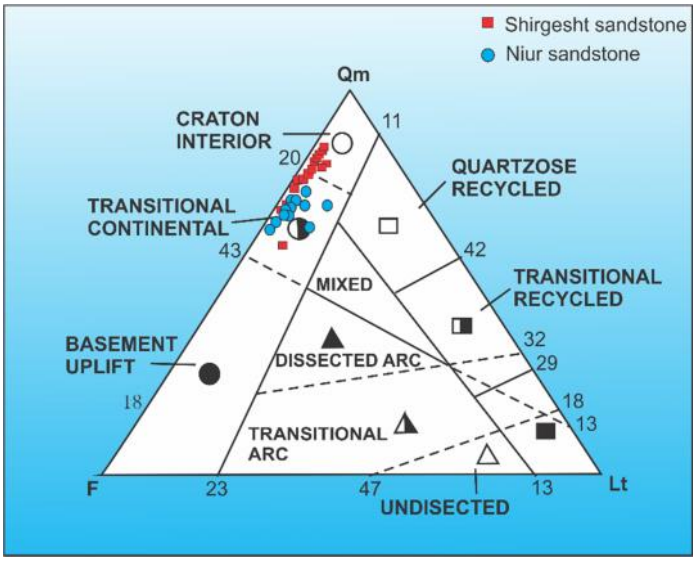

Figure 14. QFL ternary diagram (after Dickinson et al [40]). The studied samples are mainly plotted in the craton interior and transitional continental fields.

both active and passive margin margins (Fig. 16).

Paleogeography

As stated above, the UPS is composed of shale and sandstone while LPN comprises shale and carbonate rocks. Some evidences, such as greywacke sandstones and erosional basal contact as well as horizontal and cross-ripple lamination show that the UPS may have been deposited in relatively deep marine environment under turbidity currents [28]. While, hummocky, cross-ripple lamination and intraclasts in some microfacies in the LPN (Silurian) show that they may were deposited under storm conditions in shallower depth [28]. These evidences indicate gradual decreases in depth as well as reduction of turbulent conditions in the environment during deposition of these strata through time. The appearance of sandy limestone and finally limestone in LPN indicate the decreases of clastic sediments supply in comparison to deposition of the UPS during Early Silurian time. It is worthy to mention that the major lithology in UPS is sandstone, while the LPN comprises mainly limestone and shale. Therefore, these evidences

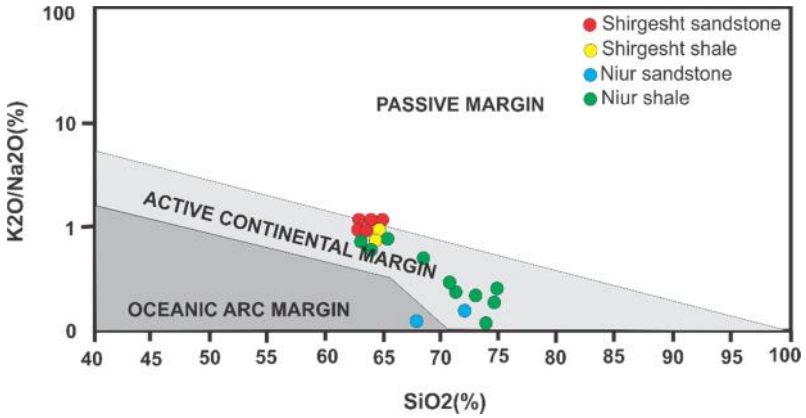

Figure 15. K_2O/Na_2O versus SiO_2 diagram illustrating active continental margin for studied samples (after Roser and Korsch [37]).

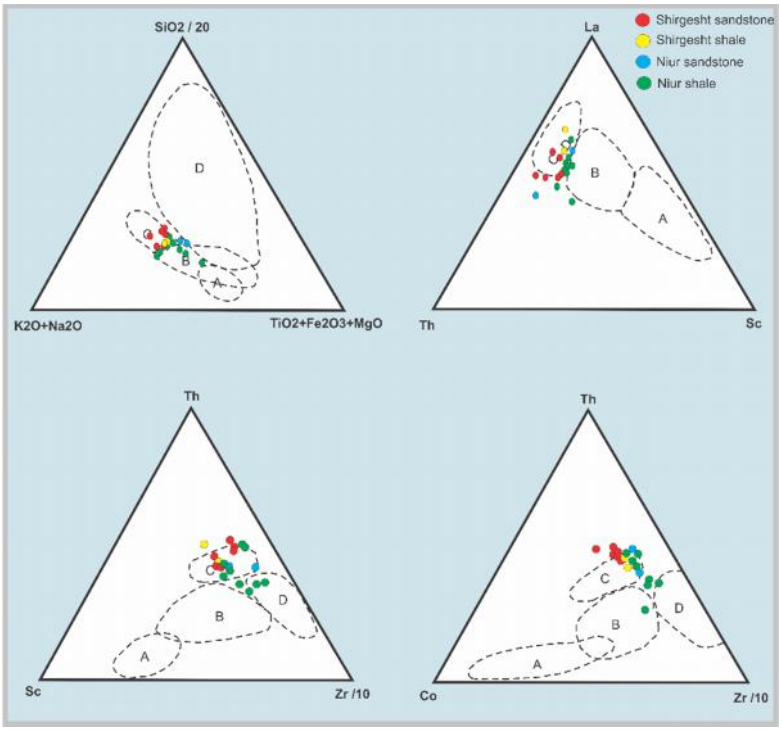

Figure 16. Tectonic discrimination ternary plots of major (after Kroonenberg [42]) and trace (after Bhatia and Crook [27]) elements for UPS and LPN formations. A: Oceanic island arc; B: Continental island arc; C: Active continental margin; D: Passive continental margin.

show establishment of the relative calm conditions of depositional environment.

The role of glaciation and its impacts on sedimentation was not clear at the region in this time. However, it is possible tectonic activities were the most important factor that controlled sedimentation at this time. Lasemi [43] interpreted depositional environment of Shirgesht Formation (deep marine influenced by turbidity currents) from tectono-sedimentary point of view and support our interpretation about the role of faults during sedimentation. He stated that deposition of the Shirghest Formation contemporaneously occurred with rifting along the normal faults (Kuhbanan-Kalmard and Naiband faults) that formed in the Central Iran. Furthermore, plot of trace and major element oxides on ternary diagrams (Fig. 16), along with field and petrography observations support our interpretation that these deposits formed in the tectonic setting, such as active and passive continental margins during deposition of the UPS and LPN, respectively. Therefore, depositional conditions can be related to the beginning of extensional phases of rifting in the studied area. This phase is compatible with rifting phase during the Early Palaeozoic (as second step) time which is related to

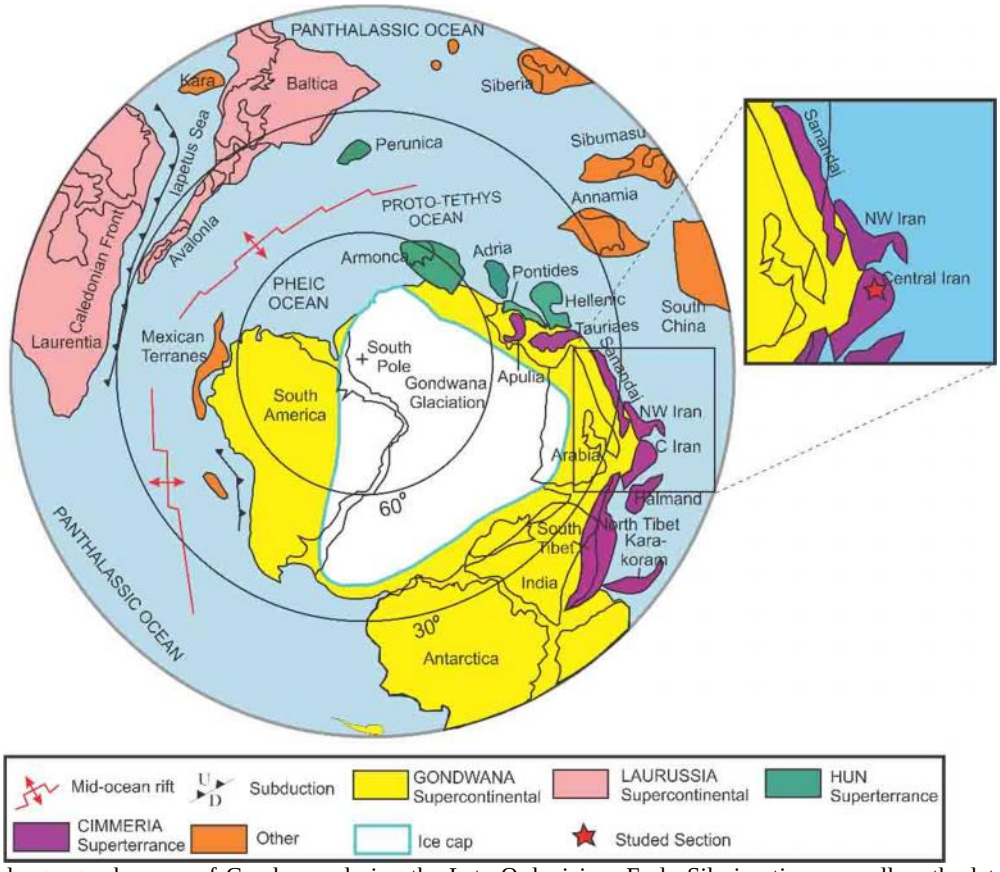

Figure 17. Paleogeography map of Gondwana during the Late Ordovician- Early Silurian time as well as the latest Hirnantian glacial phase [46]. The location of Central Iran shown on the map.

creation of the Paleo-Tethys Ocean as presented by Stampfli et al [44].

Based on petrographical and geochemical data, the felsic igneous rocks, particularly granite, were the most important source rock for UPS and LPN sandstones in the studied area. The integration of these data and our proposed rift basin, suggest that rifting created a pathway to the Tabas area for transportation of sediments from weathered older formations or basement rocks (mainly felsic igneous rocks) to depositional setting. CIA index values (65 and 74 for Shirgesht and Niur formations) and high quartz content as well as influx of clay minerals into depositional settings (greywacke petrofacies) indicate the effects of moderate to intense chemical weathering in the source area. According to CIA index values and other evidences presented before, the Central Iranian micro plate was probably located at the low paleo-latitude (in paleo-tropical range). Therefore, the temperate to semi humid climatic conditions could be dominant on Central Iran in this paleo-tropical latitude during Ordovician-Silurian time and probably rocks have undergone moderate to intense chemical weathering. Most studies show that there are facies variations in the Ordovician and Silurian deposits between the Central Iranian with Arabian plates during these periods [25], so the Central Iranian micro-plate was distinct and different from Arabian plate. Hence, our interpretation can also support the Golonka [45] illustration that microplate of Central Iran and surrounding areas were predominantly located at the paleo-latitude of less than 30° S. Although Central Iran was a part of Gondwana continent along the Paleo-Tethys Ocean during deposition of the Shirgesht (Upper Ordovician) and Niur formations (Lower Silurian) (Fig. 17).

Conclusion

The petrographic together with geochemical data have used to interpret the provenance characteristics, such as source rock, paleo-weathering of the source area, tectonic setting and finally the paleogeography of the Late Ordovician-Early Silurian time (UPS and LPN formations). The petrography studies show that sandstones have relatively high quartz content in conjunction with abundant K-feldspar grains as well as

some heavy minerals, suggesting derivation of the deposits from felsic igneous rock, particularly granite. Also the results of geochemical analysis validated this possible source rock. The mean CIA value (65 and 74 for UPS and LPN formations, respectively) as well as the plot of trace element oxides data on diagrams, such as Th/U ratio versus Th, indicates a high degree of weathering in the source area.

Our petrography and geochemical data are compatible with active and passive continental margins for UPS and LPN formations, respectively. The normal faults formed at the edge of platform during deposition of UPS Formation; therefore, as a result of rifting, sediments supply increased into the basin and deposited under turbidity currents. Furthermore, decrease of clastic sediments supply into the basin during deposition of LPN Formation indicates that deposition may took place along a passive margin during Ordovician-Early Silurian. Based on paleogeography interpretation, the UPS and LPN formations deposited during rifting stage of Paleo-Tethys in the Kuh-e-Boghou.

Acknowledgement

This paper is part of the first author's master thesis and was supported by the department of Geology, Ferdowsi University of Mashhad, Iran (research project code: 3.32816). We are grateful to all department staff for their support. We thank to reviewers for constructive comments.

References

1. Yan Z., Wang Z., Chen J., Yan Q. and Wang T. Detrital record of Neoproterozoic arc-magmatism along the NW margin of the Yangtze Block, China: U–Pb geochronology and petrography of sandstones. *J. ASI. Earth Sci.* **37**: 322–334 (2010).
2. Kundu A., Matin A. and Mukul M. Depositional environment and provenance of Middle Siwalik sediments in Tista valley, Darjiling District, Eastern Himalaya, India. *J. Earth. Syst. Sci.* **121**(1):73–89 (2012).
3. Pantoppoulos G., and Zelilidis A. Petrographic and geochemical characteristics of Paleogene turbidite deposits in the southern Aegean (Karpathos Island, SE Greece): implications for provenance and tectonic setting. *Che. der Er.* **72**:153–166 (2013).
4. Wang L., Liu C., Gao X. and Zhang H. Provenance and paleogeography of the Late Cretaceous Mengyejing Formation, Simao Basin, southeastern Tibetan Plateau: Whole-rock geochemistry, U–Pb geochronology, and Hf isotopic constraints. *Sed. Geol.* **304**: 44–58 (2014).
5. Zhang X., Pease V., Omma J. and Benedictus A. Provenance of Late Carboniferous to Jurassic sandstones for southern Taimyr, Arctic Russia: A comparison of heavy mineral analysis by optical and QEMSCAN methods. *Sed. Geol*. **329**: 166–176 (2015).
6. Zhang J., Ye T., Li S., Yuan G., Dai C., Zhang H. and Ma Y. The provenance and tectonic setting of the Lower Devonian sandstone of the Danlin Formation in southeast Yangtze Plate, with implications for the Wuyi-Yunkai orogeny in South China Block. *Sed. Geol.* **346**: 25–34 (2016).
7. Najafzadeh A., Jafarzadeh M. and Moussavi-Harami R. Provenance and tectonic setting of Upper Devonian sandstones from Ilanqareh Formation (NW Iran). *Re. Mexic. Cien. Geológ*. **27** (3): 545–561 (2010).
8. Tao H., Sun S., Wang Q., Yang X. and Jiang, L. Petrography and geochemistry of lower Carboniferous greywacke and mudstones in Northeast Junggar, China: implications for provenance, source weathering, and tectonic setting. *J. Asi. Earth Sci.* **87**: 11–25 (2014).
9. Nowrouzi Z., Moussavi-Harami R., Mahboubi A., Gharaie M.H. and Ghaemi F. Petrography and geochemistry of Silurian Niur sandstones, Derenjal Mountains, East Central Iran: implications for tectonic setting, provenance and weathering. *Arab. J. Geosci.* **7**: 2793–2813 (2014).
10. Oghenekome M.E., Chatterjee T.K., Hammond N.Q. and Bever Donker J.M. Provenance study from petrography of the late Permian – Early Triassic sandstones of the Balfour Formation Karoo Supergroup, South Africa. *J. Afr. Earth Sci.* **114**: 125–132 (2016).
11. Fatima S., Khan M.S. Petrographic and geochemical characteristics of Mesoproterozoic Kumbalgarh clastic rocks, NW Indian shield: implications for provenance, tectonic setting, and crustal evolution. *Int. Geol. Rev.* **54**: 1113–1144 (2012).
12. Armstrong-Altrin J.S., Nagarajan R., Madhavaraju J., Rosalez-Hoz L., Lee Y.I., Balaram V., Cruz-Martínez A. and Avila-Ramírez G. Geochemistry of the Jurassic and Upper Cretaceous shales from the Molango Region, Hidalgo, eastern Mexico: implications for source-area weathering, provenance, and tectonic setting. *C. R. Geosci.* **345**:185–202 (2013).
13. Zaid S.M. Provenance, diagenesis, tectonic setting and reservoir quality of the sandstones of the Kareem Formation, Gulf of Suez, Egypt. *J. Afr. Earth. Sci.* **85**:31–52 (2013).
14. Zaid S.M. Geochemistry of sandstones from the Pliocene Gabir Formation, north Marsa Alam, Red Sea, Egypt: implication for provenance, weathering and tectonic setting. *J. Afr. Earth. Sci.* **102**: 1–17 (2015).
15. Bhatia M.R. and Crook K.A.W. Trace element characteristics of greywackes and tectonic setting discrimination of sedimentary basins. *Con. Mineral. Petrol*. **92**: 181–193 (1986).
16. Purevjav N. and Roser B. Geochemistry of Devonian-Carboniferous clastic sediments of the Tsetserleg terrane, Hangay Basin, central Mongolia: provenance, source weathering, and tectonic setting. *Isl. Arc* **21**:270–287 (2012).
17. Armstrong-Altrin J.S., Nagarajan R., Lee Y.I., Kasper-Zubillaga J.J. and Córdoba-Saldaña L.P. Geochemistry of sands along the San Nicolás and San Carlos beaches, Gulf of California, Mexico: implication for provenance. *Turk. J. Earth. Sci.* **23**:533–558 (2014).

18. Xie X., O'Connor P. M. and Alsleben H. Carboniferous sediment dispersal in the Appalachian–Ouachita juncture: Provenance of selected late Mississippian sandstones in the Black Warrior Basin, Mississippi, United States. *Sed. Geol*. **342**: 191–201 (2016).
19. Ghazi S. and Mountney N. P. Petrography and provenance of the Early Permian Fluvial Warchha Sandstone, Salt Range, Pakistan. *Sed. Geol*. **233**: 88–110 (2011).
20. Abrantes Jr F.R., Nogueira A.C.R. and Soares J. L. Permian paleogeography of west-central Pangea: reconstruction using sabkhatype gypsum-bearing deposits of Parna´ıba Basin, Northern Brazil. *Sed. Geol.* **341**: 175–188 (2016).
21. Bassis A., Hinderer M. and Meinhold G. New insights into the provenance of Saudi Arabian Palaeozoic sandstones from heavy mineral analysis and single-grain geochemistry. *Sed. Geol*. **333**: 100–114 (2016).
22. Shaikh M., Lasemi Y., Aghanabati A. and Jahani D. Facies and depositional environment of Shirgesht Formation in type section, NE Tabas. *SQJG* **1**: 27–33 (2010).
23. Hairapetian V., Ghobadi Pour M., Popov L. and Modzalevskaya T.L. Stegocornu and associated brachiopods from the Silurian (Llandovery) of Central Iran. *Eston J. Earth Sci.* **61** (2): 82–104 (2012).
24. Bayatgol A. Depositional environment and diagenesis of Shirgesht Formation in Kuh-e-Asheghan and Radar, Tabas, Master *thesis*, Shahid Beheshti University, 117 p. (2011).
25. Nowrouzi Z. Moussavi-Harami R. Mahboubi A. Petrography and geochemistry of Silurian Niur sandstones, Derenjal Mountains, East Central Iran: implications for tectonic setting, provenance and weathering. *Arab J Geosci,* **7**:2793–2813 (2014).
26. Saheb Jamee S. Palinology and palinostratigraphy of deposits of member 2 in Niur Formation in SW Kashmahr at Chah-e-Tajri section, Master *thesis*, Islamic University of Iran, Mashhad Branch, 231 p. (2012).
27. Ruttner A. Nabavi M.H., Hajian J. Geology of Shirgesht area (Tabas area, East Iran). *Geological Society of Iran, Tehran,* **4**: 133p. (1968).
28. Khazaei E., Mahmoudi Gharaei M.H., Mahboubi A., Taheri J. Facies analysis in transitional from Ordovician deposits (Upper part of Shirgesht Formation) to Silurian (Lower part of Niur Formation) in SW Kashmar, North of Tabas block. *J. Geosci.* **26** (101): 111–126 (In Persian) (2016).
29. Taheri J. Geological map of the Kashmar sheet (1:100000). *Geological Survey of Iran*, 40 p. (2001).
30. Pettijohn F.J., Potter P.E., Siever R. Sand and Sandstone. *Springer-Verlag, Berlin,* 553p. (1987).
31. Taylor S.R., McLennan S.M. The Continental Crust: Its Composition and Evolution. *Blackwell Scientific Publications, Oxford,* 312 p. (1985).
32. Caracciolo L., Le Pera E., Muto F and Perri F. Sandstone petrology and mudstone geochemistry of the Peruc–Korycany Formation (Bohemian Cretaceous Basin, Czech Republic). *Int. Geo. Rev.* **53**: 1003–1031 (2011).
33. Nesbitt, H.W., Young G.M. Early Proterozoic climates and plate motions inferred from major element chemistry of lutites. *Nature.* **299**: 715–717 (1982).
34. McLennan S. M. Weathering and global denudation. *J. Geol.* **101**: 295–303 (1993).
35. Maravelis A., Zelilidis A. Petrography and geochemistry of the late Eoceneearly Oligocene submarine fans and shelf deposits on Lemnos Island, NE Greece. Implications for provenance and tectonic setting. *Geol. J.* **45**: 412–433 (2010).
36. Basu A., Young S.W., Suttner L.J., James W.C., Mack G. H. Re-evaluation of the use of adulatory extinction and polycrystallinity in detrital quartz for provenance interpretation. *J. Sediment. Petrol.* **45**: 873–882 (1975).
37. Roser B.P., Korsch, R.J. Provenance signatures of sandstone–mudstone suites determined using discriminant function analysis of major-element data. *Chem. Geol.* **67**: 119–139 (1988).
38. Cullers R.L. Implications of elemental concentrations for provenance, redox conditions, and metamorphic studies of shales and limestones near Pueblo, CO, USA. *Chemic. Geol*. **191** (4): 305–327 (2002).
39. Braccialli L., Marroni M., Pandolfi L., Rocchi S. Geochemistry and petrography of Western Tethys Cretaceous sedimentary covers (Corsica and Northern Apennines): from source areas to configuration of margins. In: Arribas J., Critelli S., Johnsson M.J. (Eds.), Sedimentary Provenance and Petrogenesis: Perspectives from Petrography and Geochemistry. *Geol. Soc. Am. Special Paper*. **420**: 73–93 (2007).
40. Dickinson W.R., Beard L.S., Brakenridge G.R., Evjavec J.L., Ferguson R.C., Inman K.F., Knepp R.A., Lindberg F.A. and Ryberg P.T. Provenance of North American Phanerozoic sandstones in relation to tectonic setting. *Geol. Soc. Am. Bull.* **94**: 222–235 (1983).
41. McLennan S. M., Taylor S. R., McCulloch M. T. and Maynard J. B. Geochemical and Nd–Sr isotopic composition of deep-sea turbidite: crustal evolution and plate tectonic associations. *Geochim. Cosmochim. Acta*. 54: 2015–2050 (1990).
42. Kroonenberg S.B. Effects of provenance, sorting and weathering on the geochemistry of fluvial sands from different tectonic and climatic environments. *Proceedings of the 29th International Geological Congress, Part A, Kyoto, Oct. 17-18:* 69-81 (1994).
43. Lasemi Y. Facies analysis, depositional environments and sequence stratigraphy of the Upper Pre-Cambrian and Paleozoic rocks of Iran. *Iran Geological Survey Publications, Tehran* 180 p. (In Persian) (2001).
44. Stampfli G. M., Raumer J. V. and Wilhem C. The distribution of Gondwana-derived terranes in the Early Paleozoic. In: Gutierrez-Marco J.C., Rabano I. and Garcia-Bellido, D. (Eds.), Ordovician of the world. Instituto Geologic y Minero de Espana, Madrid. 567–574 (2011).
45. Golonka J. Phanerozoic Paleoenvironment and Paleolithofacies Maps of Gondwana. *AGH University of Science and Technology Press. Krakow* 87p. (2012).
46. Berra F. and Angiolini L. The evolution of the Tethys region throughout the Phanerozoic: A brief tectonic reconstruction, In: Marlow L., Kendall C. and Yose L. (Eds.), Petroleum systems of the Tethyan region. *A.A.P.G. Memoir*, **106**: 1–27 (2014).